Colonies of the fungus *Aspergillus niger* are highly differentiated to adapt to local carbon source variation

Paul Daly [1], Mao Peng,[1] Hugh D. Mitchell,[2]
Young-Mo Kim,[2] Charles Ansong,[2] Heather Brewer,[3]
Peter de Gijsel,[4] Mary S. Lipton,[3] Lye Meng Markillie,[2]
Carrie D. Nicora,[2] Galya Orr,[3] Ad Wiebenga,[1]
Kristiina S. Hildén,[5] Mirjam A. Kabel,[4] Scott E. Baker,[3]
Miia R. Mäkelä [5] and Ronald P. de Vries [1,5*]

[1]*Fungal Physiology, Westerdijk Fungal Biodiversity Institute & Fungal Molecular Physiology, Utrecht University, Uppsalalaan 8, 3584 CT Utrecht, The Netherlands.*
[2]*Biological Sciences Divisions, Pacific Northwest National Laboratory, Richland, WA, 99352, USA.*
[3]*Environmental Molecular Sciences Laboratory, Pacific Northwest National Laboratory, Richland, WA, 99352, USA.*
[4]*Laboratory of Food Chemistry, Wageningen University, Bornse Weilanden 9, 6708 WG Wageningen, The Netherlands.*
[5]*Department of Microbiology, University of Helsinki, Viikinkaari 9, 00790 Helsinki, Finland.*

Summary

Saprobic fungi, such as *Aspergillus niger*, grow as colonies consisting of a network of branching and fusing hyphae that are often considered to be relatively uniform entities in which nutrients can freely move through the hyphae. In nature, different parts of a colony are often exposed to different nutrients. We have investigated, using a multi-omics approach, adaptation of *A. niger* colonies to spatially separated and compositionally different plant biomass substrates. This demonstrated a high level of intra-colony differentiation, which closely matched the locally available substrate. The part of the colony exposed to pectin-rich sugar beet pulp and to xylan-rich wheat bran showed high pectinolytic and high xylanolytic transcript and protein levels respectively. This study therefore exemplifies the high ability of fungal colonies to differentiate and adapt to local conditions, ensuring efficient use of the available nutrients, rather than maintaining a uniform physiology throughout the colony.

Introduction

Filamentous fungi grow as branching and fusing networks of mycelial hyphae, enabling them to colonize new regions of their biotope. Growth occurs by hyphal tip extension and branching (Schmieder *et al*., 2019) and involves mass flow of cytoplasm from the colony centre to the hyphal tip (Lew, 2011; Fricker *et al*., 2017). The pored septa, which partition the hyphae can be plugged with Woronin bodies (Jedd and Chua, 2000; Steinberg *et al*., 2017), bringing the potential to control molecule movement within the colony. Fusion of fungal hyphae provides interconnections within and between colonies of the same species (Glass *et al*., 2004), but the latter only occurs in young colonies, indicating that aging process reduces their compatibility with other colonies of the same species (Bleichrodt *et al*., 2015).

The connected hyphae in a colony enable cytoplasmic streaming and continuity, facilitating exchange of nutrients between different parts of the colony (Simonin *et al*., 2012). It has been hypothesized that this is due to the heterogeneity of nutrients in natural biotopes and attack by other organisms, which requires flexibility of the colony as a whole (Heaton *et al*., 2012; Guhr *et al*., 2015). No data are available about the average size of fungal colonies in nature, but they are likely to be at least several centimetres or decimetres in diameter, and possibly much larger, as the largest fungal colony discovered was as large as 965 ha (Ferguson *et al*., 2003). This leaves no doubt that the availability and composition of substrates set-upon by different parts of the fungal colony are often very different. However, the extent to which a colony adapts to its microenvironment remains unknown.

Transport of nutrients has been shown to take place over relatively long distances, when fungi were grown in environments with high and very low levels of nutrients (Bebber *et al*., 2007). In mycorrhizal fungi, there is transfer of carbon through the mycelia connecting two plants with the magnitude of the transfer increased by the carbon requirement of the receiving plant (Finlay and Read 1986;

Francis and Read 1984). These results indicate that the parts of the colony exposed to low nutrient amounts are aided by parts of the colony exposed to higher nutrient levels. However, unknown so far is whether transport of nutrients and therefore a more uniform colony physiology also occurs when different parts of the same fungal colony are in the presence of distinct nutrient-rich carbon sources.

Indications for diverse physiology within colonies have been reported, such as differences in mycelial density for a range of fungi on heterogeneous media (Olsson, 1995). Colonies of *Aspergillus niger* grown on agar plates containing either maltose or D-xylose as a carbon source showed diversity in gene expression when the periphery of the colony was compared with the centre (Levin *et al*., 2007), most likely due to carbon limitation in the centre of the colony. Growth and secretion of proteins occurred mainly in the periphery (Levin *et al*., 2007), suggesting a less active mycelium in the centre of the colony. However, in a similar study with a more complex carbon source, sugar beet pulp (SBP), growth and protein secretion were observed throughout the colony, while maintaining diversity in gene expression between the centre and periphery of the colony (Benoit *et al*., 2015a). As the composition of SBP was likely different underneath the centre, where the least recalcitrant nutrients have already been consumed, and the periphery, where the intact substrate is being digested, we hypothesize that fungal colonies adapt to the local substrate composition.

In nature, *A. niger* grows on a wide range of plant biomass and uses a diverse set of extracellular enzymes to degrade plant polysaccharides (de Vries and Visser, 2001; Pel *et al*., 2007). Most of these enzymes are classified into amino acid sequence-based families in the Carbohydrate Active enZyme (CAZy) database (www.cazy.org) (Lombard *et al*., 2014), and their production is mediated by a set of transcriptional activators, responding to specific components of plant biomass (Kowalczyk *et al*., 2014). These regulators often also control the metabolic pathways converting the released monomeric sugars (Khosravi *et al*., 2014). It can therefore be hypothesized that the different polysaccharide composition in natural biotopes will result in diverse physiology of *A. niger*, even within the colony.

In this study, we aimed to reveal the extent to which an *A. niger* colony is differentiated, when regions of the colony are exposed to different carbon sources. We compared D-glucose to SBP and wheat bran (WB) using a novel culturing method called the Pie-plate (Fig. 1), allowing comparison between pie-slice sections of a connected colony that are exposed to different nutrient-rich carbon sources. While the compartments are physically separated, the hyphae grow over these separators, connecting the mycelium in the neighbouring compartment. Both complex substrates contain significant amounts of

cellulose, but they differ in the other polysaccharides. WB contains hardly any pectin and its main hemicellulose is (arabino-)xylan. In contrast, SBP is rich in pectin, while the D-xylosyl residues detected in SBP (Table 1) originate mainly from the complex pectic molecules and the hemicellulose xyloglucan. Therefore, these two complex plant biomass substrates require different enzyme sets for their degradation (van den Brink and de Vries, 2011) and different catabolic pathways to convert the released monosaccharides (Khosravi *et al*., 2014).

We addressed differentiation within the colony at the transcriptomic, proteomic and metabolomic level. Our results showed that *A. niger* colonies adapt to the local substrate, producing significantly different extracellular enzyme sets and activating diverse metabolic pathways, corresponding to the composition of these different nutritious environments.

Results

Global clustering of the molecular responses revealed a differentiating colony across a broad range of physiological processes

Aspergillus niger was cultured on Pie-plates containing three spatially separated substrates, D-glucose, WB and SBP (Fig. 1 and Supporting Information Fig. S1). Overall growth appeared highly similar on all three compounds, with the exception of the production of a yellow pigment in the WB compartments. We observed this pigment also in other cultures and conditions (data not shown), but the nature of it is not known. Analysis of the colony was performed at the transcriptomic, proteomic and metabolomic level, to capture the dynamic nature of the colony's physiology. Principal component analysis of the transcriptome, exo- and intra-proteome, and exo- and intra-metabolome revealed a highly differentiated colony, in which the compartments with the same substrate clustered together (Supporting Information Fig. S2). The compartments surrounded by the same substrate in general separated more clearly from each other than the intermediate compartments. Therefore, we focused on these compartments (G2, S2 and W2) for subsequent detailed analysis of the colony.

The differences in abundance of transcripts and proteins between G2, S2 and W2 demonstrated broad physiological differences across the colony. When the total set of genes was considered, a relatively small percentage of them (between 3% and 10%) was significantly upregulated or downregulated (Fig. 2A and Supporting Information Dataset S1B–D). In contrast, a higher percentage of CAZy genes related to plant biomass degradation was upregulated on the plant biomass substrates compared with D-glucose (21%–25%, Fig. 2A, Supporting
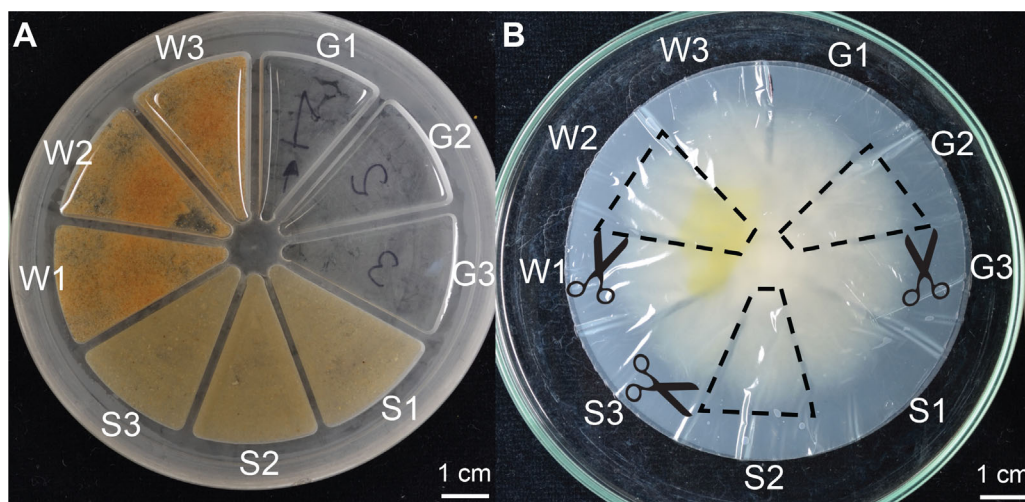
Fig. 1. The Pie-plate cultivation setup. A. Pie-plate where three adjacent compartments were filled with the same substrate. B. Image of an *A. niger* colony grown between two perforated polycarbonate membranes. Dotted lines indicate the part of the mycelia that was sampled above each compartment. While all nine compartments were sampled, detailed analysis was conducted from the central compartment on each of the substrates. G1-G3 = ᴅ-glucose. S1-S3 = sugar beet pulp (SBP), W1-W3 = wheat bran (WB). See Supporting Information Fig. S1 for microscopy images of colony. [Color figure can be viewed at wileyonlinelibrary.com]

Information Dataset S1F–H). A similar pattern was observed for the intracellular proteomics data set, with only 1.8%–5.2% significantly upregulated or down-regulated proteins, when all detected proteins were considered. In contrast, 7%–15% of the sugar catabolic enzymes were more abundant on the plant biomass substrates compared with ᴅ-glucose (Fig. 2A and Supporting Information Dataset S2).

Analysis of gene ontology (GO) term enrichment confirmed this high level of differentiation (Fig. 2B and Supporting Information Dataset S3). Enriched GO terms with respect to upregulated genes on the crude substrates compared with ᴅ-glucose included oxidoreductase activity, transmembrane transport, lipid catabolic process, carbohydrate metabolic process and transport, and hydrolase activity towards *O*-glycosyl compounds, while GO terms for catechol metabolic process were only enriched on W2 compared with G2 (Fig. 2B). In contrast, GO term aspartic acid-

type endopeptidase activity was enriched in G2 compared with S2, as was GO term tricarboxylic acid cycle (Fig. 2B). Similarly, the GO terms cellular amino acid biosynthetic process and glycolysis were enriched in transcripts that were higher in G2 compared with W2. Interestingly, GO term cellular amino acid biosynthetic process was also enriched in S2 compared with W2. This could be due to differences in protein availability in the substrates with no protein supplied in the ᴅ-glucose compartments, while the protein content of WB (15%) (Balandrán-Quintana *et al.*, 2015) is approximately twice that of SBP (8%) (Kühnel *et al.*, 2011). This would also explain the enrichment of the GO term aspartic acid-type endopeptidase activity on WB compared with SBP, as higher proteolysis on WB would reduce the need for amino acid synthesis. Differentiation was not restricted to GO terms directly related to carbohydrates but was observed across a wide range of physiological functions (Supporting Information Dataset S3).

Table 1. Sugar beet pulp and WB composition before and after *A. niger* cultivation. The carbohydrates (presented as anhydro) were measured from acid hydrolysates of the substrates in the central compartment of the Pie-plate taken before and after culturing with *A. niger* ($n = 3$).

Carbohydrates (Mol% ± SE)	Sugar beet pulp		Wheat bran	
	Before	After	Before	After
Glucose	51 ± 1.7	73.6 ± 1.2	37.5 ± 0.9	31.4 ± 0.2
Arabinose	26.2 ± 0.5	7.3 ± 1.1	19.9 ± 0.3	28.5 ± 0.1
Xylose	3.5 ± 0.0	5.1 ± 0.4	39.4 ± 0.5	35.4 ± 0.3
Galactose	8.7 ± 0.1	5.4 ± 0.2	1.2 ± 0.0	1.8 ± 0.1
Galacturonic acid	5.6 ± 0.7	3 ± 0.4	1 ± 0.1	1.2 ± 0.0
Mannose	2.2 ± 0.1	3.2 ± 0.0	0.3 ± 0.0	0.8 ± 0.1
Rhamnose	1.7 ± 0.8	1.2 ± 0.1	ND	ND
Glucuronic acid	0.7 ± 0.1	0.8 ± 0.02	0.3 ± 0.1	0.4 ± 0.0

ND = not detected.
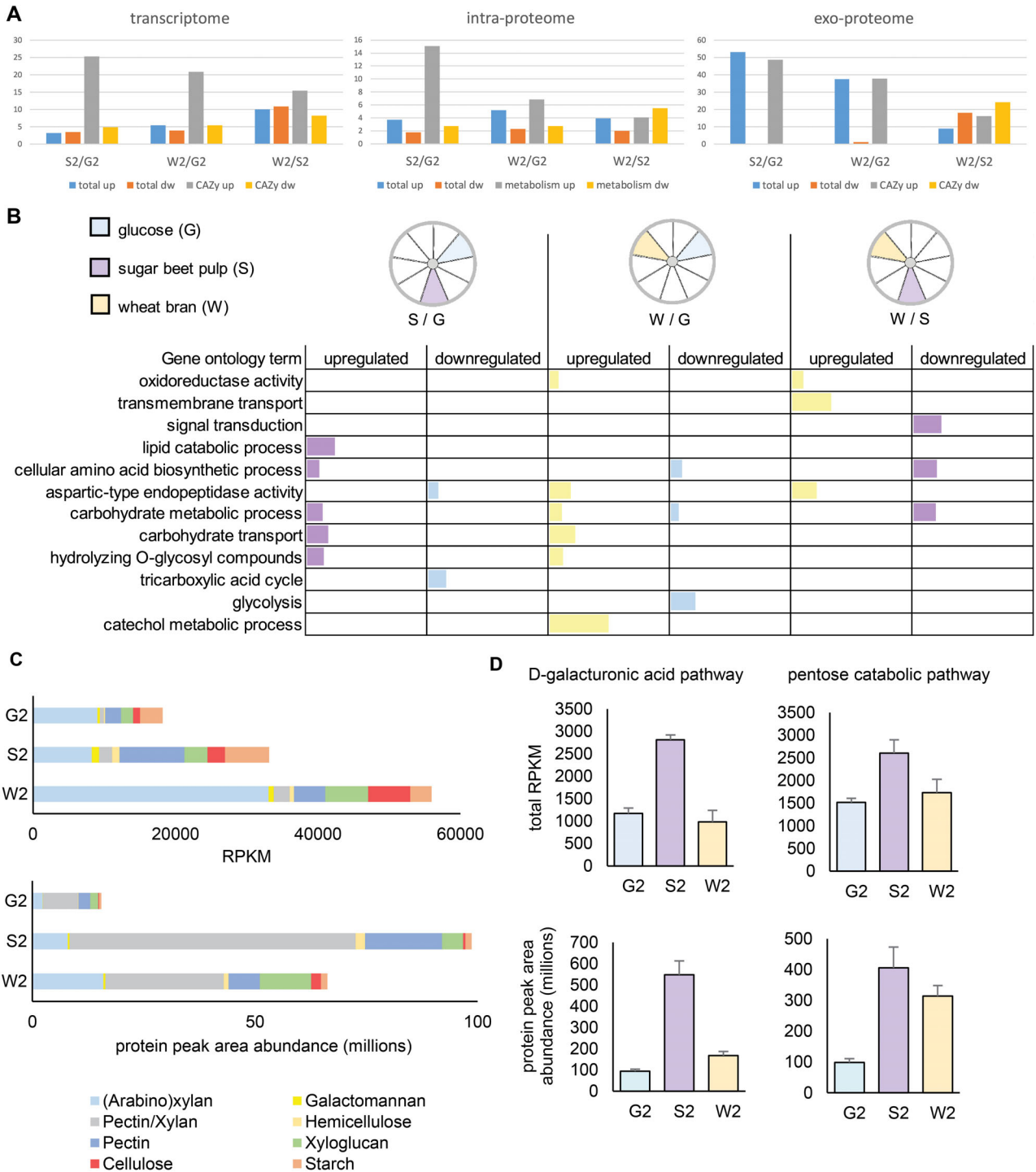
Fig. 2. Transcriptome and proteomic analysis of differentiation within the *A. niger* colony. A. Percentage of averaged differentially upregulated and downregulated genes and proteins in the total data set and specific subsets. B. Selection of enriched GO terms in the differentially expressed transcripts from comparisons of the central compartments. The size of the coloured bar indicates the proportion of the total transcripts annotated with an enriched GO term that were present in the upregulated or downregulated transcripts. These terms demonstrate the broad range of biological functions contributing to the differentiation of the colony. See Supporting Information Dataset S3 for complete list of enriched GO terms. C. Summary of transcript and exo-protein abundances of CAZymes according to the substrate they degrade. D. Transcript and intracellular protein abundances of carbon catabolic pathways which catabolize sugars that differ in abundance between the substrates. Error bars represent standard errors. [Color figure can be viewed at wileyonlinelibrary.com]

log₂ of abundance values — RNAseq (0–14), exo-proteome (0–25)

Gene ID	CAZy	Activity	Substrate	Cluster
07501	CE12	RGAE	Pectin	1
02023	GH31	AXL	Xyloglucan	
09612	GH2	MND	Galactomannan	
00965	PL1_4	PEL	Pectin	
00952	CBM48 – GH13_8	GBA	N/A	
02123	GH13_25 – GH133	GDB	N/A	
11747	GH27 – CBM13	AGL	Galactomannan	
08807	GH2	GUS	Not annotated	
00263	GH28	PGA	Pectin	
00475	GH31	AGD	Starch	
07382	GH95	AFC	Xyloglucan	
00953	GH28	RHG	Pectin	
07699	GH13_1	AMY	Starch	
10881	GH43	BXL	(Arabino)xylan	
07248	GH5_12	EGL	Cellulose	2
07089	GH95	AFC	Xyloglucan	
05201	GH13_40	AGD	Starch	
02571	GH28	PGA	Pectin	
01606	GH51	ABF	Pectin/Xylan	
00839	GH105	URH	Pectin	3
09976	GH1	BGL	Cellulose	
09051	GH2	MND	Galactomannan	
05252	CE8	PME	Pectin	4
08805	GH28	PGA	Pectin	
08281	GH28	PGX	Pectin	
05260	GH28	PGX	Pectin	
11738	GH35	LAC	Pectin	
09644	GH3	BGL	Cellulose	5
04608	GH43	ABN	Pectin	
10498	GH5_9	EXG	Pectin	
09890	GH43	BXL	(Arabino)xylan	
03736	GH3	BGL	Cellulose	
00016	GH36	AGL	Galactomannan	
10808	GH5_23	EXG	Pectin	
04153	PL1_4	PEL	Pectin	
00431	N/A	FAE	Pectin/Xylan	
07975	GH1	BGL	Cellulose	
08767	PL1_4	PEL	Pectin	
02162	GH78	RHA	Pectin	
01071	GH35	LAC	Pectin	
09530	GH5_9	EXG	Pectin	
06141	GH43	ABN	Pectin	
09810	GH28	PGX	Pectin	
04196	GH26	MAN	Galactomannan	6
08392	GH12	XG-EGL	Xyloglucan	
01739	GH88	UGH	Pectin	7
02479	GH35	LAC	Pectin	
10115	PL4_3	RGL	Pectin	
01737	GH27	AGL	Galactomannan	
08325	CE8	PME	Pectin	
08631	GH28	RGX	Pectin	
06244	GH43	BXL	(Arabino)xylan	
00684	PL4_1	RGL	Pectin	
06419	GH3	BXL/ABF	(Arabino)xylan	
02832	GH28	RGX	Pectin	
03595	GH32	SUC	Inulin	
08018	GH36	AGL	Galactomannan	
09126	GH28	RHG	Pectin	
01787	GH74 – CBM1	XG-EGL	Xyloglucan	8
10870	GH6	CBH	Cellulose	
08912	GH5	MAN	Galactomannan	
02451	GH3	BXL	(Arabino)xylan	9
02931	CE	FAE	Pectin/Xylan	
06316	AA8 – AA3_1	CDH	Cellulose	10
09019	CBM1 – GH6	CBH	Cellulose	
03383	AA9	LPMO	Cellulose	
10133	GH3	BGL	Cellulose	11
02585	GH5_5 – CBM1	EGL	Cellulose	
06053	CE16	Not annotated	Hemicellulose	12
06782	GH28	PGA	Pectin	
02524	GH31	AGD	Starch	
10449	GH3	BGL	Cellulose	
07094	GH43	ABN	Pectin	
01069	GH67	AGU	(Arabino)xylan	
07469	GH28	XGH	Pectin	
08517	GH1	BGL	Cellulose	
11105	GH131	ML-EGL	Cellulose	13
11147	AA9	LPMO	Cellulose	
03087	GH32	INX	Inulin	
03929	AA9 – CBM1	LPMO	Cellulose	
10643	GH53	GAL	Pectin	14
03144	GH28	PGX	Pectin	
02835	GH28	PGA	Pectin	
10559	GH28	RGX	Pectin	
10558	GH78	RHA	Pectin	
00743	GH27 – CBM35	AGL	Galactomannan	
05859	GH28	PGA	Pectin	15
07700	GH31	AGD	Starch	
00268	GH31	AXL	Xyloglucan	
06379	CE16	Not annotated	Hemicellulose	
03768	GH54 – CBM42	ABF	Pectin/Xylan	
06791	GH5_5 – CBM1	EGL	Cellulose	
11773	GH43 – CBM35	BXL	(Arabino)xylan	
08701	GH5_16	GLN	Pectin	
02827	GH11	XLN	(Arabino)xylan	
00814	AA9 – CBM1	LPMO	Cellulose	16
10865	GH51	ABF	Pectin/Xylan	
02630	GH35	LAC	Pectin	
07470	CE8	PME	Pectin	
04916	CE16	Not annotated	Hemicellulose	17
00169	CE12	RGAE	Pectin	
04917	GH5_5	EGL	Cellulose	
00092	GH43	ABN	Pectin	
01918	GH12	XG-EGL	Xyloglucan	18
03339	CE1	AXE	(Arabino)xylan	
08708	GH10	XLN	(Arabino)xylan	
05407	GH43	ABN	Pectin	
00819	GH12	XG-EGL	Xyloglucan	
03928	GH11	XLN	(Arabino)xylan	
09875	GH13_1 – CBM20	AMY	Starch	19
04000	GH28	PGA	Pectin	
05358	GH27	AGL	Galactomannan	
04953	GH7	CBH	Cellulose	20
08380	GH12	XG-EGL	Xyloglucan	
00007	CE	FAE	Pectin/Xylan	
02584	GH7 – CBM1	CBH	Cellulose	21
08707	GH62	AXH	(Arabino)xylan	
01648	GH11	XLN	(Arabino)xylan	
08300	GH15 – CBM20	GLA	Starch	

As we only varied the carbon source in the compartments, in our detailed analysis in the next sections, we focused on gene groups that are related to extracellular degradation of these carbon sources to monomeric sugars, sugar uptake and sugar metabolism.

Differentiation in the colony matches the substrate-specific required functions

Plant polysaccharide degrading CAZymes are highly specific for their substrate and linkage, and therefore fungi produce different sets of CAZymes depending on the substrate composition. Our results show that different parts of a single colony, only a few centimetres apart and exposed to different plant biomass substrates, are able to locally produce a well-suited enzyme set. There were overall more polysaccharide degrading CAZyme encoding genes expressed in the S2 (124), compared to W2 (108) and D-glucose (97). This correlated well with the substrate composition, which was obvious when the genes were divided into polysaccharide-related CAZy-groups, and the reads per kilobase million (RPKM) values and extracellular protein abundance were then summed up per group (Fig. 2C). The transcriptome and exo-proteome of the colony exposed to WB are dominated by xylanolytic genes. In contrast, pectinolytic genes represented a larger proportion of total expression values on SBP, which was confirmed by measuring selected enzyme activities (Supporting Information Fig. S3). This reflects the high abundance of xylan and pectin in WB and SBP, respectively (Table 1). The degradation of both substrates over the course of the cultivation also matches the production of these enzyme sets as indicated by the changes in the proportions of sugars in the acid hydrolysates of the solids after culturing (Table 1).

Hierarchical clustering of the expression levels and protein abundance of CAZymes acting on plant biomass confirmed this overall pattern and demonstrated a set of mainly pectinolytic and amylolytic genes/enzymes that were specifically upregulated in S2 (Fig. 3, Clusters 1–4, 7, 14). As the higher levels of the pectinolytic genes/ enzymes can be explained by the high level of pectin in SBP, the higher level of amylolytic genes suggests the presence of significant amounts of starch/maltose or sucrose in SBP. These result in activation of the

Fig. 3. Hierarchical clustering, using Euclidian distance, of transcript levels of plant biomass degrading CAZymes from mycelia growing on the central compartment on glucose (G), sugar beet pulp (S) or wheat bran (W). The vertical grey dotted line shows the cut-off used to delineate the clusters, which are numbered 1–21. The CAZymes are colour-coded according to nine substrate groups that they putatively act on. The protein abundance from exo-proteome is shown adjacent to the transcript. See Supporting Information Dataset S1 for explanation of the abbreviations used for activities. [Color figure can be viewed at wileyonlinelibrary.com]

amylolytic transcriptional activator AmyR, which, however, can also be activated by low levels of D-glucose (vanKuyk *et al*., 2012). Similarly, higher expression level and protein abundance was observed for xylanolytic and cellulolytic genes/proteins on WB (Fig. 3, Clusters 8–11). High diversity was also observed for the sugar metabolic pathways, although for these the diversity was higher at the proteomic than at the transcriptomic level (Supporting Information Fig. S4 and Dataset S1 and S2).

The part of the colony grown on SBP showed a clear specialization towards pectin conversion

The genes or proteins differentially expressed or produced in the part of the colony grown on SBP included half of the 64 *A. niger* pectin-specific CAZy genes or CAZymes (Martens-Uzunova and Schaap, 2009). The total pectinolytic gene expression in the colony positively correlated with the amount of pectin in the locally available substrate, being highest on SBP followed by WB and D-glucose (Fig. 2C). In addition, 29 out of 46 and 23 out of 31 of the significantly higher expressed plant biomass degradation related CAZy genes on S2 versus G2 and W2, respectively, encode pectinolytic activities (Supporting Information Dataset S1F,H). Similarly, 12 out of 18 and 7 out of 9 of the plant biomass degradation related CAZymes with a higher abundance in S2 compared with G2 and W2, respectively, are pectinolytic enzymes (Supporting Information Dataset S5F,H).

After release from pectin by *A. niger*, D-galacturonic acid and L-rhamnose are catabolized via the D-galacturonic acid pathway, involving four genes (*gaaA*, *gaaB*, *gaaC* and *larA*), and the L-rhamnose pathway, involving three genes (*lraA*, *lraB* and *lraC*) respectively (Khosravi *et al*., 2014). The highest total expression of the D-galacturonic acid pathway genes was in the SBP part of the colony (Fig. 2D top panel), and the four significantly higher expressed sugar catabolism related genes in S2 compared to G2 were all related to D-galacturonic acid or L-rhamnose metabolism (Dataset 1J). All four D-galacturonic acid-related catabolic enzymes were significantly more abundant in S2 compared with G2 or W2 (Fig. 2D bottom panel, Dataset 2F and H). Most of the sugar catabolic enzymes detected in higher abundance in S2 compared with G2 were related to D-galacturonic acid or L-arabinose catabolism (Dataset 2F).

The part of the colony exposed to WB displayed the highest xylanase expression and production

Hemicellulolytic and cellulolytic transcripts and enzymes are activated by the transcriptional activator XlnR in response to the presence of D-xylose in *A. niger* (Gruben *et al*., 2017), which is an abundant building block of the WB xylan (Table 1). The total expression of these transcripts in W2 was approximately fivefold higher than in S2 or G2 (Fig. 2C). In addition, 24 out of 38 and 22 out of 28 of the significantly higher expressed plant biomass degradation related CAZy genes on W2 versus G2 and S2, respectively, encode (hemi-)cellulolytic activities (Dataset 1G,H). Exo-proteomics also identified (hemi-)cellulolytic enzymes at higher levels in W2 compared with S2 and G2 (Dataset 5G,H). These included an endoxylanase (NRRL3_01648/XlnB), a β-xylosidase (NRRL3_02451/XlnD), an endoglucanase (NRRL3_06791/EglB) and a cellobiohydrolase (NRRL3_02584/CbhB).

Pentose catabolism is more prominent in parts of the colony growing on pentoses

The pentose catabolic pathway (PCP) converts D-xylose and L-arabinose via five enzymatic conversions, all of which were detected in the intracellular proteomics from the *A. niger* colony (Supporting Information Dataset S2). L-arabinose was preferentially consumed in SBP parts of the colony as its level decreased more than that of the other sugars present in SBP (D-galacturonic acid, L-rhamnose, and D-galactose) during cultivation (Table 1). Compared to G2, the abundance of three PCP enzymes related to L-arabinose conversion (LarA, LarB, LxrA) was significantly higher in S2, and two PCP enzymes (XyrA, XkiA) were higher in W2, while XdhA had higher abundance on both S2 and W2 (Fig. 2D and Dataset 2F,G). However, there was no clear localized expression of the PCP genes (Fig. 2D top panel and Supporting Information Dataset S1 and S2). The localization at the protein but not transcript level for the PCP highlights the temporally dynamic nature of the physiology in the *A. niger* colony.

The end-products of the PCP and the D-galacturonic acid pathway will enter the central glycolysis pathway, which also converts D-glucose originating from cellulose. Corresponding with the general need for this pathway, most of the glycolytic transcripts and proteins were expressed and produced at similar levels throughout the colony (Supporting Information Fig. S3 and Dataset S1 and S2). The GO term for glycolysis (GO:0006096) was only enriched in the transcripts that were higher in the part of the colony on D-glucose compared to WB (Supporting Information Dataset S3) likely reflecting the far higher concentrations of D-glucose initially present in this compartment.

Discussion

In this study, we aimed to determine the extent to which different parts of a fungal colony adapt to locally available carbon sources and as such evaluate the physiological

differentiation within fungal colonies. The ability for a colony to differentiate would make sense in a natural setting, where fungal colonies can extend over significant distances while being exposed to a highly heterogeneous substrate profile. Maintaining a uniform physiology under such conditions would require extensive intracolony transport of nutrients, generating a significant energetic burden for the colony, especially if this is dependent on active transport. A previous study in the mushroom forming basidiomycete fungus *Agaricus bisporus* provided evidence for highly specific transport of sugars from the vegetative mycelium to the fruiting body (Patyshakuliyeva *et al*., 2013), arguing against passive diffusion as the mechanism for intracolony sugar transport.

Most studies addressing nutrient transport in colonies focused on the difference between nutrient rich and nutrient poor (starvation) areas (Olsson, 1995; Bebber *et al*., 2007; van Peer *et al*., 2009). This does not consider what would happen if different parts of a colony are growing in nutrient-rich areas, but with a different substrate composition, which is also a common situation in nature. We tested this situation by exposing different parts of *A. niger* colonies to WB, SBP and D-glucose, respectively, and showed that there was a high level of adaptation to these locally available substrates. Instead of a constant level throughout the colony, we observed locally differentiated levels of gene expression and enzyme production that matched the requirements for the degradation and catabolism of the prevalent polysaccharides. This was particularly apparent for the higher levels of pectinolytic genes and enzymes on SBP, which is rich in pectin, and for the higher levels of xylanolytic genes and enzymes on WB, which is rich in xylan (Table 1). In addition, the genes and proteins of the intracellular sugar catabolic pathways matched the monomeric sugars present in the prominent locally present polysaccharides. This was especially obvious for the D-galacturonic acid and L-rhamnose pathway on SBP, which is the only substrate tested here that contained L-rhamnose. However, also the PCP enzyme levels showed an adaptation to the substrates with the L-arabinose-related PCP enzymes being especially induced on SBP, in which L-arabinose is abundantly present as short-side chains (29). On WB, which is higher in D-xylose, the three PCP enzymes needed for D-xylose conversion were significantly induced. This correlates well with the amount of free extracellular arabinose and xylose that was present in the SBP and WB compartments (Supporting Information Fig. S5). We did observe a gradual increase in some enzyme activities towards the neighbouring substrate (Supporting Information Fig. S3), which could indicate a moderate transfer of signal molecules through the mycelium. However, this can also be explained by leakage of media components into the neighbouring compartment when the polycarbonate membranes are applied to the pie plate. This possible leakage was the main reason to focus predominantly on the middle compartments in this study.

The observed differentiation indicated that under our conditions, there were limits to cytoplasmic flow within the colony, thus preventing a more uniform physiology. In a previous study where *A. niger* was grown on a simple sugar, cytoplasmic streaming in older parts of the colony was limited due to their multicellular nature (Bleichrodt *et al*., 2015), which is likely also the case in our study considering the culturing time. In our setup, we do not just compare the young mycelium at the periphery at the colony, but whole sections of the colony from the periphery to the centre. Some studies have suggested that only the periphery is the growing part of the colony (Wösten *et al*., 1991; Levin *et al*., 2007), but these studies were based on conditions in which soluble sugars were used that were often already depleted in the centre of the colony. However, we have shown more recently that during growth on complex carbon sources, *A. niger* has actively growing mycelium throughout the colony (Benoit *et al*., 2015a), generating an active and complex multicellularity in the colony. This multicellular nature and the observed diversity within the colony could be facilitated by Woronin bodies plugging the septal pores. Therefore, future studies in which mutant strains such as Δ*hexA* (Jedd and Chua, 2000; Bleichrodt *et al*., 2015), which lacks Woronin bodies, are included would provide further insight into the importance of these structures for colony differentiation.

Our results demonstrate that the presence of a nutritious substrate in each part of the colony prevents extensive flow of nutrients through the colony, as also evidenced by the diversity in intracellular metabolic profiles, unlike what was observed when exposing some parts of the colony to nutrient starvation (Bebber *et al*., 2007). These two situations therefore represent different colony physiologies and highlight the highly flexible nature of fungal colonies that enables them to select the most appropriate solution to the prevalent environmental conditions. This however does not mean that no movement of nutrients occurred in our experimental setup. The part of the colony growing on D-glucose also showed higher transcript levels of plant biomass degrading CAZymes than expected from a culture where only D-glucose was present even if that D-glucose had been mostly consumed (Daly *et al*., 2017) and extracellular CAZymes were identified in the compartments where D-glucose was the substrate. However, we cannot rule out contribution of a low level of sugars that appear to diffuse into an adjacent compartment (Supporting Information Fig. S5).

The lower diversity in localized transcriptomic compared to proteomic response, especially for the (hemi-) cellulose degrading proteins secreted into the WB

compared with D-glucose compartment (Fig. 2C) and for the intracellular pathways (Fig. 2D), could be due to post-transcriptional or post-translational regulation (Sachs, 1998) of these transcripts and enzymes. Another contributing factor could be the initial CreA-mediated (Ruijter *et al.*, 1997) repression in the D-glucose compartments delaying the protein production. As the levels would be significantly lower at the moment of sampling (~1 mM), the transcript levels may have already adapted to the non-repressing condition, while this was not yet the case for the protein levels.

A major driver for the localized response of the fungal colony is the local availability of inducing compounds (typically monomeric sugars) that activate transcriptional regulators, which in turn drive the expression of their specific target gene sets (Benocci *et al.*, 2017). D-xylose is the major inducer of (hemi-)cellulases in *A. niger* (Gruben *et al.*, 2017), which explains why the cellulolytic transcripts and proteins were higher in the WB part of the colony as it contains more D-xylosyl residues (WB) even though both WB and SBP contain substantial amounts of cellulose. In contrast, while L-arabinose is mainly an inducer of pectinolytic genes (de Vries *et al.*, 2002; Gruben *et al.*, 2017) it is a major component of both WB (in arabinoxylan) and SBP (in pectin) (Table 1). This contributed to the induction of pectinolytic genes and enzymes on WB despite them not being needed to degrade WB. Nevertheless, this cross-talk by inducers did not prevent a predominantly locally adapted response of enzymes that are required for the degradation of the available polysaccharides.

The highly differentiated localized response in the relatively small colonies of our study highlights the ability of *A. niger* to adapt and tune gene expression to fit its local carbon sources. This ability implies an evolutionary process that may have selected for tailored responses to substrate composition within parts of a single colony growing on plant biomass of spatially heterogeneous composition, as this may provide a competitive advantage over other microorganisms. Whether such a high level of diversity is only shared with other generalist fungi or is a common process also found in fungi with a more specialized biotope or substrate profile remains to be studied. It is clear however, that the transport of nutrients within fungal colonies is highly dependent on the nutritional state of the local environment. As previously reported, when comparing local environments under nutritious and starvation conditions, transport of nutrients can be observed through significant parts of the colony (Olsson, 1995; Bebber *et al.*, 2007). However, our study demonstrates that when separate parts of the colony are exposed to different, but equally nutritious conditions, nutrient transport appears to be highly limited and the parts of the colony display a highly differentiated physiology, closely matching the locally present nutrients.

Experimental procedures

Culturing conditions and sampling

Aspergillus niger N402 (Bos *et al.*, 1988) was used throughout this study. To inoculate pre-cultures, conidia were harvested from a complete medium (de Vries *et al.*, 2004) agar plate containing 1% w/v D-fructose and 1000 conidia in 2 μl of water were inoculated onto a perforated polycarbonate (PC) membrane on a minimal medium (de Vries *et al.*, 2004) agar plates with 25 mM D-fructose. After overnight incubation at 30°C, a second PC membrane was applied on top of the pre-culture and the incubation at 30°C continued with a total incubation time of 3 days when the colony grew to a diameter of ~1.5–2 cm. The pre-culture sandwich was transferred to a Pie-plate (Fig. 1), which had three consecutive compartments filled with MM supplemented with either 1% w/v D-glucose, SBP or WB. The Pie-plates were incubated at 30°C for 3.5 days (see Supporting Information Fig. S1 for images of colony at time of sampling). The mycelia growing on each of the compartments was sampled by cutting through the PC membrane along the boundary of the compartment with a scalpel blade and then the PC membrane was peeled away before transferring the mycelia to a 2 ml tube and flash freezing in liquid nitrogen. Samples were isolated from biological triplicates for RNA, protein and metabolite extractions.

RNA, protein and metabolite extractions

For RNA and intracellular metabolites and protein extraction, the mycelia were ground using a TissueLyser (Qiagen). The RNA was extracted and checked for quality as described previously (Benoit *et al.*, 2015a). Intracellular proteins and metabolites were released from the ground mycelia using 500 μl of extraction buffer (50 mM potassium phosphate buffer pH 7, 5 mM $MgCl_2$, 5 mM β-mercaptoethanol and 0.5 mM EDTA) with inversion of the tube followed by centrifugation (20 000 × *g*, 4°C and 5 min), before mixing 300 μl of the supernatant with 1.5 ml of cold 2:1 (v/v) chloroform: methanol. The rest of the procedure was described previously (Daly *et al.*, 2018).

Carbohydrate composition analysis

The solids from the G2, S2 and W2 from replicate plates were pooled and analysed alongside un-inoculated controls. Carbohydrate content and composition were determined in duplicate by modification of the method of Englyst and Cummings (Englyst and Cummings, 1984), which was described previously (van Erven *et al.*, 2017). The absolute amounts of uronic acids are underestimated as the heating of the solids at 90°C as well as

autoclaving, likely led to the degradation of a proportion of the uronic acids.

RNA library preparation, sequencing and data processing

For RNA-Seq, the SMARTer[R] Ultra™ Low RNA kit was used to generate a full-length cDNA template library, followed by use of the Ion Plus fragment library kit (Thermo Fisher Scientific) to fragment cDNA and barcode adapter ligation for template preparation. The template library was quantified using the Ion Library TaqMan™ Quantitation Kit (Thermo Fisher Scientific). The emulsion clonal bead amplification to generate bead templates for Ion Torrent platform was performed using the Ion PI™ Hi-Q™ Chef Kit (Thermo Fisher Scientific) with Ion PI™ Chip Kit v3 (Thermo Fisher Scientific) on the Ion Chef System (Thermo Fisher Scientific). Sequencing was performed using the Ion PI™ Hi-Q™ Sequencing 200 Kit (Thermo Fisher Scientific) on the Ion Proton sequencer with sequencing data processing using the Torrent Suite ™ Software (Ver. 4.0.2) on the Torrent server.

Data quality was assessed with htseq-qa (Kim *et al.*, 2008). Reads were aligned to the *A. niger* NRRL3 genome (Aguilar-Pontes *et al.*, 2018) using TMAP 3.0.1, with the − g parameter set to 0 and the − a parameter set to 1. The RNAseq data set was deposited at the GEO (Barrett *et al.*, 2013) database under the accession number GSE118894. BAM file outputs were mapped to genes using htseq-count (Anders *et al.*, 2015) using default settings. Differential expression and principal component (multi-dimensional scaling) analyses were conducted using the R package DESeq2 (Love *et al.*, 2014). The analysis was performed on three independent biological replicates.

Genes with an RPKM ≤6 were considered lowly expressed and genes were considered differentially expressed if the DESeq2 log$_2$ fold change was >1 or < −1, P_{adj} < 0.05 and the RPKM was >6 in the relevant condition. Hierarchical clustering on the expressed PBD CAZy using the log2 RPKM values (+1) was performed in the R statistical environment using the gplots package with Euclidian distance and complete linkage. The gene ontology (GO) annotations were retrieved from JGI MycoCosm, https://genome.jgi.doe.gov/Aspni_NRRL3_1/Aspni_NRRL3_1.home.html. The GO terms enriched within the significant differential expressed gene list compared with the genome background was detected using a hypergeometric distribution model. GO terms were considered enriched when *P* value <0.05, the number of *A. niger* proteins annotated with the GO term >2 and the number of proteins annotated with the GO term in the list of significantly higher or lower expressed or transcripts >1. The PBD CAZy substrate and enzyme annotations

were based on the studies by Benoit *et al.* (2015b), Gruben *et al.* (2017), and Kowalczyk *et al.* (2017)).

Proteomics data generation and analysis

The intracellular proteome was analysed using equal amounts of proteins from each sample and normalized for total signal intensity, whereas the extracellular proteins collected from the liquid in the compartments was analysed using equivalent volumes of liquid without any normalization for total signal intensity. Sample preparation was performed as previously described (Daly *et al.*, 2018). The intracellular samples were all diluted to a concentration of 0.1 μg μL^{-1} in water for analysis by LC–MS as described previously (Daly *et al.*, 2018). In order to analyse the extracellular samples using equivalent volumes from each compartment, the highest concentrated sample was identified in the extracellular sample set and it was diluted to 0.1 μg μL^{-1} and the remainder of the set was diluted using the same volumes as this sample.

MS analysis was performed using a Q-Exactive Plus mass spectrometer (Thermo Scientific) outfitted with a homemade nano-electrospray ionization interface. Electrospray emitters were homemade using 150 μm o. d. × 20 μm i.d. chemically etched fused silica (Kelly *et al.*, 2006). The ion transfer tube temperature and spray voltage were 250°C and 2.2 kV, respectively. Data were collected for 120 min following a 10 min delay after completion of sample trapping and start of gradient. FT-MS spectra were acquired from 300 to 1800 m/z at a resolution of 30 k (AGC target 3e6) and while the top 12 FT-HCD-MS/MS spectra were acquired in data-dependent mode with an isolation window of 2.0 m/z and at a resolution of 17.5 k (AGC target 1e5) using a normalized collision energy of 32 and a 30 s exclusion time.

Generated MS/MS spectra were searched using the mass spectral generating function plus (MSGF+) algorithm (Kim *et al.*, 2008; Kim and Pevzner, 2014) against the *A. niger* translated genome sequence available from Aspni_NRRL3_1 (Aguilar-Pontes *et al.*, 2018). Identified peptides of at least six amino acids in length having MSGF scores ≤1E^{-10}, which corresponds to an estimated false discovery rate (FDR) < 1% at the peptide level, were used to generate an accurate mass and time (AMT) tag database (Zimmer *et al.*, 2006). Matched peptide features from each LC–MS data set were then filtered on a FDR of less than or equal to 5% using the Statistical Tools for AMT tag confidence metric (Stanley *et al.*, 2011). When a peptide is identified by the AMT tag approach, its relative abundance can be determined by calculating the area under the curve of the peptide ion peak in the MS measurement. For the intracellular proteomic data set, the relative peptide abundance measurements were normalized using mean centring in DAnTE

(Polpitiya *et al*., 2008) whereas the exo-proteomics data set was not subject to mean centering. Peptide abundance values were then rolled up to proteins using RRollup function in DAnTE, a minimum of three peptides was required for the Grubb's outlier test for outlying peptides, with a *P* value cut-off of 0.05. Furthermore, for a protein to be considered present in a condition, an abundance measurement in at least two of the replicates for that condition was required. For an identified protein to be considered significantly differentially produced, the requirements were a $\log_2$ fold change of the mean intensity values of >1 or < -1 and $P < 0.05$ from a two-tailed homoscedastic (assuming equal variances) *t*-test of the $\log_2$ transformed intensity values. Note that where an intensity value was not detected for a protein in a sample, a zero value was used ($\log_2$ of 1). Proteins were categorized as higher (which can include only present in one of the conditions), not significantly different or not present in comparisons of the central compartments (CCs) on each of the substrates. The PCAs were performed on the log intensity values of all proteins from the exo- and intracellular proteomics data sets using FactoMineR version 1.39 (Lê *et al*., 2008) in R version 3.4.3. GO enrichment was performed as for the RNAseq data set described previously. The mass spectrometry proteomics data have been deposited to the ProteomeXchange Consortium via the PRIDE (Vizcaino *et al*., 2016) partner repository with the data set identifier PXD010431 (10.6019/PXD010431).

Metabolomics data generation and analysis

The aqueous phase, containing the polar metabolites, obtained from the chloroform:methanol extractions was processed for using GC–MS-based metabolomics data generation and analysis using pipelines described previously (Daly *et al*., 2018; Khosravi *et al*., 2018). MetaboAnalyst (Xia *et al*., 2015) was used for the principal component analysis of the metabolite abundances.

Enzymatic assays

Samples were assayed for enzymatic activity towards four *para*-nitrophenol (*p*NP) linked substrates (*p*-nitrophenyl α-ʟ-arabinofuranoside, *p*-nitrophenyl α-ᴅ-galactopyranoside, *p*-nitrophenyl β-ᴅ-galactopyranoside and *p*-nitrophenyl β-ᴅ-xylopyranoside) at a final concentration of 0.01% w/v. The 100 μl reactions were incubated between 3 and 4 h at 30°C in 25 mM sodium acetate buffer pH 5.0. The reactions were terminated with 100 μl 0.25 M Na_2CO_3 and absorbance read at 405 nm using a Fluostar OPTIMA plate reader (BMG Labtech). The activity was expressed as nmol pNP $\cdot$ min^{-1} $\cdot$ mL^{-1} and the data were presented as the averaged value of the biological triplicate samples.

Sugar analysis of compartments after culturing

Enzymes present in the supernatants collected from the compartments were heat inactivated at 99°C for 5 min before sugar analysis of the liquids to avoid further conversion of the sugars. ʟ-arabinose, ᴅ-glucose, ᴅ-xylose and ᴅ-galacturonic acid were measured using a Dionex HPAEC-PAD (Dionex ICS-5000+ system; Thermo Scientific) system with the program for measuring the monosaccharides as described previously (Mäkelä *et al*., 2016).

Data availability

The raw RNAseq data have been deposited at the GEO database under the accession number GSE118894. The mass spectrometry proteomics data have been deposited at the ProteomeXchange Consortium via the PRIDE partner repository with the dataset identifier PXD010431.

References

Aguilar-Pontes, M.V., Brandl, J., McDonnell, E., Strasser, K., Nguyen, T.T.M., Riley, R., *et al*. (2018) The gold-standard genome of *Aspergillus Niger* NRRL 3 enables a detailed view of the diversity of sugar catabolism in fungi. *Stud Mycol* **91**: 61–78.

Anders, S., Pyl, P.T., and Huber, W. (2015) HTSeq-a python framework to work with high-throughput sequencing data. *Bioinformatics* **31**: 166–169.

Balandrán-Quintana, R.R., Mercado-Ruiz, J.N., and Mendoza-Wilson, A.M. (2015) Wheat bran proteins: a review of their uses and potential. *Food Rev Int* **31**: 279–293.

Barrett, T., Wilhite, S.E., Ledoux, P., Evangelista, C., Kim, I. F., Tomashevsky, M., *et al*. (2013) NCBI GEO: archive for functional genomics data sets-update. *Nucleic Acids Res* **41**: D991–D995.

Bebber, D.P., Hynes, J., Darrah, P.R., Boddy, L., and Fricker, M.D. (2007) Biological solutions to transport network design. *Proc Biol Sci* **274**: 2307–2315.

Benocci, T., Aguilar-Pontes, M.V., Zhou, M., Seiboth, B., and de Vries, R.P. (2017) Regulators of plant biomass degradation in ascomycetous fungi. *Biotechnol Biofuels* **10**: 152.

Benoit, I., Zhou, M., Vivas-Duarte, D.A., Downes, D., Todd, R.B., Kloezen, W., *et al*. (2015a) Spatial

differentiation of gene expression in *Aspergillus Niger* colony grown for sugar beet pulp utilization. *Sci Rep* **5**: 13592.

Benoit, I., Culleton, H., Zhou, M., DiFalco, M., Aguilar-Osorio, G., Battaglia, E., *et al*. (2015b) Closely related fungi employ diverse enzymatic strategies to degrade plant biomass. *Biotechnol Biofuels* **8**: 1–14.

Bleichrodt, R.-J., Hulsman, M., Wösten, H.A.B., and Reinders, M.J.T. (2015) Switching from a unicellular to multicellular organization in an *Aspergillus Niger* hypha. *MBio* **6**: e00111.

Bos, C., Debets, A.J.M., Swart, K., Huybers, A., Kobus, G., and Slakhorst, S.M. (1988) Genetic analysis and the construction of master strains for assignment of genes to six linkage groups in *Aspergillus Niger*. *Curr Genet* **14**: 437–443.

Daly, P., van Munster, J.M., Blythe, M.J., Ibbett, R., Kokolski, M., Gaddipati, S., *et al*. (2017) Expression of *Aspergillus Niger* CAZymes is determined by compositional changes in wheat straw generated by hydrothermal or ionic liquid pretreatments. *Biotechnol Biofuels* **10**: 35.

Daly, P., Casado López, S., Peng, M., Lancefield, C.S., Purvine, S.O., Kim, Y.-M., *et al*. (2018) *Dichomitus squalens* partially tailors its molecular responses to the composition of solid wood. *Environ Microbiol* **20**: 4141–4156.

de Vries, R.P., and Visser, J. (2001) *Aspergillus* enzymes involved in degradation of plant cell wall polysaccharides. *Microbiol Mol Biol Rev* **65**: 497–522.

de Vries, R.P., Jansen, J., Aguilar, G., Pařenicová, L., Benen, J.A.E., Joosten, V., *et al*. (2002) Expression profiling of pectinolytic genes from *Aspergillus Niger*. *FEBS Lett* **530**: 41–47.

de Vries, R.P., Burgers, K., van de Vondervoort, P.J.I., Frisvad, J.C., Samson, R.A., and Visser, J. (2004) A new black *Aspergillus* species, *A. vadensis*, is a promising host for homologous and heterologous protein production. *Appl Environ Microbiol* **70**: 3954–3959.

Englyst, H.N., and Cummings, J.H. (1984) Simplified method for the measurement of total non-starch polysaccharides by gas-liquid chromatography of constituent sugars as alditol acetates. *Analyst* **109**: 937–942.

Ferguson, B.A., Dreisbach, T.A., Parks, C.G., Filip, G.M., and Schmitt, C.L. (2003) Coarse-scale population structure of pathogenic *Armillaria* species in a mixed-conifer forest in the Blue Mountains of Northeast Oregon. *Can J For Res* **33**: 612–623.

Finlay, R.D., and Read, D.J. (1986) The structure and function of the vegetative mycelium of ectomycorrhizal plants. I. Translocation of ^{14}C-labelled carbon between plants interconnected by a common mycelium. *New Phytol* **102**: 143–156.

Francis, R., and Read, D.J. (1984) Direct transfer of carbon between plants connected by vesicular–arbuscular mycorrhizal mycelium. *Nature* **307**: 53–56.

Fricker, M.D., Heaton, L.L.M., Jones, N.S., and Boddy, L. (2017) The mycelium as a network. *Microbiol Spectr* **5**: 32.

Glass, N.L., Rasmussen, C., Roca, M.G., and Read, N.D. (2004) Hyphal homing fusion and mycelial interconnectedness. *Trends Microbiol* **12**: 135–141.

Gruben, B.S., Mäkelä, M.R., Kowalczyk, J.E., Zhou, M., Benoit-Gelber, I., and de Vries, R.P. (2017) Expression-based clustering of CAZyme-encoding genes of *Aspergillus Niger*. *BMC Genomics* **18**: 900.

Guhr, A., Borken, W., Spohn, M., and Matzner, E. (2015) Redistribution of soil water by a saprotrophic fungus enhances carbon mineralization. *Proc Natl Acad Sci U S A* **112**: 14647–14651.

Heaton, L., Obara, B., Grau, V., Jones, N., Nakagaki, T., Boddy, L., and Fricker, M.D. (2012) Analysis of fungal networks. *Fungal Biol Rev* **26**: 12–29.

Jedd, G., and Chua, N.-H. (2000) A new self-assembled peroxisomal vesicle required for efficient resealing of the plasma membrane. *Nat Cell Biol* **2**: 226–231.

Kelly, R.T., Page, J.S., Luo, Q., Moore, R.J., Orton, D.J., Tang, K., and Smith, R.D. (2006) Chemically etched open tubular and monolithic emitters for nanoelectrospray ionization mass spectrometry. *Anal Chem* **78**: 7796–7801.

Khosravi, C., Benocci, T., Battaglia, E., Benoit, I., and de Vries, R.P. (2014) Sugar catabolism in *Aspergillus* and other fungi related to the utilization of plant biomass. *Adv Appl Microbiol* **90**: 1–28.

Khosravi, C., Battaglia, E., Dalhuijsen, S., Visser, J., Aguilar-Pontes, M.V., Zhou, M., *et al*. (2018) Blocking hexose entry into glycolysis activates alternative metabolic conversion of these sugars and upregulates pentose metabolism in *Aspergillus nidulans*. *BMC Genomics* **19**: 214.

Kim, S., Gupta, N., and Pevzner, P.A. (2008) Spectral probabilities and generating functions of tandem mass spectra: a strike against decoy databases. *J Proteome Res* **7**: 3354–3363.

Kim, S., and Pevzner, P.A. (2014) MS-GF+ makes progress towards a universal database search tool for proteomics. *Nature Commun* **5**: 5277.

Kowalczyk, J.E., Benoit, I., and de Vries, R.P. (2014) Regulation of plant biomass utilization in *Aspergillus*. *Adv Appl Microbiol* **88**: 31–56.

Kowalczyk, J.E., Lubbers, R.J.M., Peng, M., Battaglia, E., Visser, J., and de Vries, R.P. (2017) Combinatorial control of gene expression in *Aspergillus Niger* grown on sugar beet pectin. *Sci Rep* **7**: 12356.

Kühnel, S., Schols, H.A., and Gruppen, H. (2011) Aiming for the complete utilization of sugar-beet pulp: examination of the effects of mild acid and hydrothermal pretreatment followed by enzymatic digestion. *Biotechnol Biofuels* **4**: 14.

Lê, S., Josse, J., and Husson, F. (2008) FactoMineR: an R package for multivariate analysis. *J Stat Software* **25**: 18.

Levin, A.M., de Vries, R.P., Conesa, A., de Bekker, C., Talon, M., Menke, H.H., *et al*. (2007) Spatial differentiation in the vegetative mycelium of *Aspergillus Niger*. *Eukaryot Cell* **6**: 2311–2322.

Lew, R.R. (2011) How does a hypha grow? The biophysics of pressurized growth in fungi. *Nat Rev Microbiol* **9**: 509–518.

Lombard, V., Golaconda Ramulu, H., Drula, E., Coutinho, P. M., and Henrissat, B. (2014) The carbohydrate-active enzymes database (CAZy) in (2013). *Nucleic Acids Res* **42**: D490–D495.

Love, M., Huber, W., and Anders, S. (2014) Moderated estimation of fold change and dispersion for RNA-seq data with DESeq2. *Genome Biol* **15**: 550.

Mäkelä, M.R., Mansouri, S., Wiebenga, A., Rytioja, J., de Vries, R.P., and Hildén, K. (2016) *Penicillium subrubescens* is a promising alternative for *Aspergillus Niger* in enzymatic plant biomass saccharification. *N Biotechnol* **33**: 834–841.

Martens-Uzunova, E.S., and Schaap, P.J. (2009) Assessment of the pectin degrading enzyme network of *Aspergillus Niger* by functional genomics. *Fungal Genet Biol* **46**: S170–S179.

Olsson, S. (1995) Mycelial density profiles of fungi on heterogeneous media and their interpretation in terms of nutrient reallocation patterns. *Mycol Res* **99**: 143–153.

Patyshakuliyeva, A., Jurak, E., Kohler, A., Baker, A., Battaglia, E., de Bruijn, W., *et al*. (2013) Carbohydrate utilization and metabolism is highly differentiated in *Agaricus bisporus*. *BMC Genomics* **14**: 663.

Pel, H.J., de Winde, J.H., Archer, D.B., Dyer, P.S., Hofmann, G., Schaap, P.J., *et al*. (2007) Genome sequencing and analysis of the versatile cell factory *Aspergillus Niger* CBS 513. *Nat Biotech* **25**: 221–231.

Polpitiya, A.D., Qian, W.-J., Jaitly, N., Petyuk, V.A., Adkins, J.N., Camp, D.G., *et al*. (2008) DAnTE: a statistical tool for quantitative analysis of -omics data. *Bioinformatics* **24**: 1556–1558.

Ruijter, G.J., Vanhanen, S.A., Gielkens, M.M., van de Vondervoort, P.J., and Visser, J. (1997) Isolation of *Aspergillus Niger creA* mutants and effects of the mutations on expression of arabinases and L-arabinose catabolic enzymes. *Microbiol* **143**: 2991–2998.

Sachs, M.S. (1998) Posttranscriptional control of gene expression in filamentous fungi. *Fungal Genet Biol* **23**: 117–125.

Schmieder, S.S., Stanley, C.E., Rzepiela, A., van Swaay, D., Sabotic, J., Norrelykke, S.F., *et al*. (2019) Bidirectional propagation of signals and nutrients in fungal networks via specialized hyphae. *Curr Biol* **29**: 217–228.

Simonin, A., Palma-Guerrero, J., Fricker, M., and Glass, N.L. (2012) Physiological significance of network organization in fungi. *Eukaryot Cell* **11**: 1345–1352.

Stanley, J.R., Adkins, J.N., Slysz, G.W., Monroe, M.E., Purvine, S. O., Karpievitch, Y.V., *et al*. (2011) A statistical method for assessing peptide identification confidence in accurate mass and time tag proteomics. *Anal Chem* **83**: 6135–6140.

Steinberg, G., Harmer, N.J., Schuster, M., and Kilaru, S. (2017) Woronin body-based sealing of septal pores. *Fungal Genet Biol* **109**: 53–55.

van den Brink, J., and Vries, R.P. (2011) Fungal enzyme sets for plant polysaccharide degradation. *Appl Microbiol Biotechnol* **91**: 1477–1492.

van Erven, G., de Visser, R., Merkx, D.W.H., Strolenberg, W., de Gijsel, P., Gruppen, H., and Kabel, M. A. (2017) Quantification of lignin and its structural features in plant biomass using ^{13}C lignin as internal standard for pyrolysis-GC-SIM-MS. *Anal Chem* **89**: 10907–10916.

van Peer, A.F., Müller, W.H., Boekhout, T., Lugones, L.G., and Wösten, H.A.B. (2009) Cytoplasmic continuity revisited: closure of septa of the filamentous fungus *Schizophyllum commune* in response to environmental conditions. *PLoS one* **4**: e5977.

vanKuyk, P.A., Benen, J.A., Wösten, H.A., Visser, J., and de Vries, R.P. (2012) A broader role for AmyR in *Aspergillus Niger*: regulation of the utilisation of D-glucose or D-galactose containing oligo- and polysaccharides. *Appl Microbiol Biotechnol* **93**: 285–293.

Vizcaino, J.A., Csordas, A., del-Toro, N., Dianes, J.A., Griss, J., Lavidas, I., *et al*. (2016) 2016 update of the PRIDE database and its related tools. *Nucleic Acids Res* **44**: D447–D456.

Wösten, H.A., Moukha, S.M., Sietsma, J.H., and Wessels, J.G. (1991) Localization of growth and secretion of proteins in *Aspergillus Niger*. *J Gen Microbiol* **137**: 2017–2023.

Xia, J., Sinelnikov, I.V., Han, B., and Wishart, D.S. (2015) MetaboAnalyst 3.0-making metabolomics more meaningful. *Nucleic Acids Res* **43**: W251–W257.

Zimmer, J.S., Monroe, M.E., Qian, W.J., and Smith, R.D. (2006) Advances in proteomics data analysis and display using an accurate mass and time tag approach. *Mass Spectrom Rev* **25**: 450–482.

Supporting Information

Additional Supporting Information may be found in the online version of this article at the publisher's web-site:

Figure S1. Brightfield microscopy images of an *A. niger* colony at time of sampling (after peeling off upper polycarbonate membrane) on the Pie-plate separator between adjacent substrates of either (A) wheat bran (W3) and D-glucose (G1), (B) D-glucose (G3) and sugar beet pulp (S1) or (C) sugar beet pulp (S3) and wheat bran (W1).

Figure S2. Principal component analysis of the (A) transcripts, (B) extracellular proteins, (C) intracellular proteins and (D) extracellular identified metabolites from sections of an *A. niger* colony growing on D-glucose (G), sugar beet pulp (S) or wheat bran (B). The three compartments of the Pie-plate containing the same substrate are numbered 1, 2 and 3 in a clockwise direction. The samples from the central compartment (2) on each substrate are highlighted. Dim = dimension.

Figure S3. Exo-enzymatic activities measured towards the *p*-nitrophenol substrates for β-xylosidase, β-galactosidase, α-galactosidase and α-arabinofuranosidase from compartments containing either D-glucose (G), sugar beet pulp (S) or wheat bran (W) on which an *A. niger* colony was growing. Error bars represent standard errors from biological duplicates.

Figure S4. Hierarchical clustering, using Euclidian distance, of transcript levels of carbon catabolic enzymes and selected characterized transporters sampled from *A. niger* mycelia growing on the central compartment on glucose (G), sugar beet pulp (S) or wheat bran (W). The vertical grey dotted line shows the cut-off used to delineate the clusters. The pathways and transporters are colour-coded except for genes involved in multiple pathways. The protein abundance from the intracellular proteome is shown adjacent to the transcript.

Figure S5. Arabinose, glucose, xylose and galacturonic acid concentrations at the time of sampling (after 4 d) in the compartments on which *A. niger* was growing. Error bars

represent standard errors from biological duplicates. G = D-glucose, S = sugar beet pulp and W = wheat bran.

Dataset S1. Transcriptome dataset from the mycelial sections of an *A. niger* colony growing on compartments containing D-glucose (G2), sugar beet pulp (S2) or wheat bran (W2).

Dataset S2. Intracellular proteome dataset from the mycelial sections of an *A. niger* colony growing on compartments containing D-glucose (G2), sugar beet pulp (S2) or wheat bran (W2).

Dataset S3. Summary of gene ontology (GO) terms enriched in the significantly different transcripts from at least one of the pair-wise comparisons of the central compartments containing D-glucose (G2), sugar beet pulp (S2) or wheat bran (W2).

Dataset S4. Analysis of exo- and intracellular metabolites. (A) Aqueous exo-metabolites from the liquid in the compartments containing D-glucose (G), sugar beet pulp (S) or wheat bran (W) on which an *A. niger* colony was growing as well as controls of sugar beet pulp and wheat bran that were not inoculated with *A. niger*. (B) Aqueous intracellular metabolites from *A. niger* mycelia growing on the compartments containing D-glucose (G), sugar beet pulp (S) or wheat bran (W).

Dataset S5. Exo-proteome dataset from the liquid in the compartments containing D-glucose (G2), sugar beet pulp (S2) or wheat bran (W2) on which an *A. niger* colony was growing.